



Investigations on Wear Behaviour of AISI 4140 Hot Strip Mill Roller Hardfaced with Martensitic Stainless Steel by Submerged Arc Welding Process

R.V. Patel^{a,*}, S.P. Wanare^a, V.D. Kalyankar^a

^aMechanical Engineering Department, Sardar Vallabhbhai National Institute of Technology, Surat, 395007, Gujarat, India.

Keywords:

Submerged arc welding
Hardfacing
Multilayer
Abrasive wear resistance
Hardness
Hot strip mill roller

ABSTRACT

In the present investigation, a worn-out hot strip mill roller of AISI 4140 material has been reconditioned by the deposition of hardfacing. The roller belongs to Arcelormittal Nippon Steel India, which is used to transfer metallic strip. This roller is continuously subjected to wear due to the oxide scale on the slab surface. Its regular maintenance and repair cause significant production loss. Therefore, two hardfacings of martensitic stainless steels with different composition are deposited on the surface of AISI 4140 steel by submerged arc welding and comparative analysis is performed to achieve the superior wear resistance. Further, hardfaced samples are evaluated on the basis of abrasive wear test, hardness, microstructure and worn-out morphology. The results showed that the hardfacing with combination of large volume fraction of martensite and small volume fraction of residual austenite attained the highest value of hardness up to 380 HV whereas the reverse combination showed 332 HV hardness and the minimum mass loss is observed for sample with 380 HV hardness. At the end, the most suitable material for the hardfacing of AISI 4140 is suggested. The outcomes of this work would be beneficial to improve the service life of roller of hot strip mill.

* Corresponding author:

Ronakkumar Visabhai Patel 
E-mail: ronakvp3011@gmail.com

Received: 11 August 2020
Revised: 13 November 2020
Accepted: 31 January 2021

© 2021 Published by Faculty of Engineering

1. INTRODUCTION

Steel making is a technologically demanding and challenging process during which a significant amount of wear occurs on the steel product handling equipments. Several factors affect the functionality of these parts. Among them, some of the factors are abrasive wear, adhesive wear, erosive wear, thermal fatigue, corrosion, residual stresses, etc [1]. For smooth functioning

of steel process plant, it is necessary to regularly perform inspection and maintenance activities. Roller is an essential part of a steel process plant. During its continuous servicing, its diameter decreases by wear due to oxide scale on the slab surface which further results in its ineffective functionality [2]. Hence, it is necessary to either replace the roller or to increase the diameter of roller by depositing material on it so that it can be used again.

Among these two, the approach of reconditioning of the roller by hardfacing can bring about a significant reduction in the annual consumption cost of the roller and also increases its efficiency [3]. It will reduce the expenditure incurred on the purchase of new rollers and also reduces the production losses.

Weld hardfacing techniques are widely adopted to deposit a highly wear resistant layer on the substrate to improve its abrasive and corrosive wear resistance [4,5]. Various processes such as gas tungsten arc welding (GTAW), gas metal arc welding (GMAW), plasma transferred arc welding (PTAW), shielded metal arc welding (SMAW), laser welding and submerged arc welding (SAW) have been used for deposition of highly wear resistant hardfacing on the rollers [5-8]. Among these advanced techniques, SAW is a widely adopted process in the industry because of its higher deposition rate, high welding speed, better surface appearance, high melting power and lower cost [5,9,10]. Several researchers have performed studies by using SAW process for hardfacing [5,11,12].

Martensitic stainless steels possess excellent wear resistance and found to be the superior option for hardfacing of hot strip mill roller [13]. Vinas et al. [11] have examined the degradation of deposited layers on continuous caster rolls to identify the tribological properties of rolls and concluded that the abrasive and the adhesive wear resistance of rolls increases because of the presence of passivated chromium in the weld metal. Du Toit and Van Niekerk [12] have analyzed the effect of post weld heat treatment (PWHT) on mechanical properties and microstructural changes of martensitic stainless steels, which is used for hardfacing the continuous caster rollers and proposed that the deposited layer satisfies the minimum hardness requirement with a minimal level of retained austenite and carbide precipitation. Zhang et al. [14] have analyzed the microstructure and volume of retained austenite in 13Cr-4Ni (C=0.05 wt. %) martensitic stainless steel during intercritical tempering and found that as the intercritical tempering holding time increases, the volume of retained austenite initially increases, reaches a maximum value and finally decreases.

AISI 4140 steel has been widely used in aerospace, automotive and manufacturing industries such as bolts, sprockets, spindles, gears and drilling collars [15-18]. These components are used in several tribological environments which led to adhesive or abrasive wear. Many researchers and steel manufacturing companies consider AISI 4140 as a roller material because it provides wear resistance, corrosion resistance, high impact toughness, hardness and yield strength [11,13,19].

In this study, a worn-out AISI 4140 steel roller with radial dimension loss of 9 mm is reconditioned by depositing two different hardfacings of martensitic stainless steel having different composition using SAW process to obtain higher wear resistance than substrate material. Further, these roller samples are subjected to wear test, hardness, analysis of microstructure and analysis of worn-out morphology at different thicknesses of 4, 6.5 and 9 mm to investigate the influence of hardfacing thickness. A slurry abrasive wear test is conducted to evaluate the three-body abrasive wear phenomena that occur on the surface of a roller. On the basis of the results, the most suitable material between the two is suggested for hardfacing of hot strip mill roller.

2. MATERIALS AND METHODS

2.1 Materials

The chemical compositions of substrate material and hardfacing wires used in the present investigation are presented in Table 1.

These hardfacing wires are available in the market which has 3.2 mm diameter. The H1 is manufactured by Welding Alloy and its grade is CHROME CORE 414-N. The H2 is manufactured by Bohler and its grade is SK-C 742N. Flux used during SAW process is made of a composition of SiO₂-TiO₂-CaO-MgO-Al₂O₃-MnO-CaF₂. These grade wires are specially designed to resist abrasive wear, impact load, corrosion, etc. with high temperature sustainability [20,21]. These overlay materials are also suitable for hardfacing of continuous caster rolls, hardfacing of hot rolling, pressure vessel for petroleum and nuclear power plant, support rollers of large drum-type heating surface, steam generator, hydraulic cylinder piston rod, ball valves and power transmission components in shipbuilding.

Table 1. Chemical composition of materials under consideration

Material	Chemical composition (wt. %)							
	C	Mn	Mo	Cr	Ni	Si	N	V
AISI 4140 (Substrate)	0.4	0.85	0.25	1	-	0.25	-	-
Hardfacing wire 1 (H1)	0.08	1	0.5	13.5	4.3	0.6	0.1	-
Hardfacing wire 2 (H2)	0.05	1.5	1.5	12	3.5	-	0.1	0.2

2.2 Execution of experiments

SAW under direct current reversed polarity was employed for deposition of hardfacings. The welding conditions are as follows: welding voltage 30-35 V, welding current 420-460 A, wire extension 15-20 mm, welding speed 10-12 meter/hour and overlap rate was 8-12 % of hardfaced layer width. Turning process is performed before deposition of hardfacing to remove cracks, uneven roundness, foreign particles on the surface of the roller, etc. Further, the die penetration test is performed to check the quality of surface as shown in Fig. 1.

**Fig. 1.** Die penetration tested roller

Now, AISI 4140 steel is prone to cracking due to its poor weldability therefore preheating is very essential to avoid cracks and PWHT also require in order to relieving the stress. Now, the carbon content and alloy content of the substrate metal are two major factors that affect preheat temperature and also, the substrate material has martensite transformation temperature range between 280°C to 350°C. Therefore, to prevent substrate material from cracks, preheating of roller is carried out at 250°C as shown in Fig. 2 and maintained as an interpass temperature throughout the hardfacing of roller as shown in Fig. 3. Three multi-track layers are deposited on the substrate material having thicknesses of approximately 3.5 mm each. Similar procedure is followed for both the hardfacings.

**Fig. 2.** Preheating of the roller**Fig. 3.** Hardfacing process of roller

PWHT produces tempered martensite which is accepted as an ideal combination of strength and toughness for hot strip mill roller. Therefore, PWHT of hardfaced roller is carried out with heating of roller for 12 hours up to 580°C temperatures. Later on, the soaking of the roller is carried out for 8 hours to achieve a uniform temperature throughout the roller thickness. It is then followed by furnace cooling to reach up to the room temperature, which takes around 8 hours. Further, the hardfaced portion of the roller is cut-down for sample preparation as shown in Fig. 4.

**Fig. 4.** Cut down portion of hardfaced roller

As shown in Fig. 5, the hardfaced portion of the roller is cut down further into a rectangular shape. In Fig. 5, there are three samples of each H1 hardfacing and H2 hardfacing. Samples are prepared with different thicknesses to analyze wear resistance and hardness properties at different thicknesses of hardfaced surface as shown in Fig. 6.



Fig. 5. Samples cut from the roller

The influence of hardfacing material thickness on hardness and wear resistance of prepared samples is investigated over three different thicknesses, i.e., 4 mm, 6.5 mm and 9 mm for both the type of hardfacings.

Layer 3 (H1-3)	Layer 3 (H2-3)
Layer 2 (H1-2)	Layer 2 (H2-2)
Layer 1 (H1-1)	Layer 1 (H2-1)
Substrate (AISI 4140)	Substrate (AISI 4140)

Fig. 6. Schematic diagram of H1 and H2 hardfacing samples

When the roller is in service condition, oxide scales are formed on the surface of slab. In order to remove oxide scales, water is sprayed frequently on the slab. During the spray of water on the slab, the mixture of scale and water are formed. When this mixture come in contact with the slab and roller, it forms three-body abrasion, which is very much similar to ASTM G105 standard [2,22,23]. The parameters used during wear tests are specimen size $(25.4 \pm 0.8 \text{ mm}) \times (57.2 \pm 0.8 \text{ mm}) \times (6.4 \text{ to } 15.9 \text{ mm})$, Test load 222N, Test time 1000 revolutions, RPM 245 rpm, Sand AFS 50/70. The hardness values of different hardfacing deposits are measured on Vicker's hardness testing machine using a 10 kgf load. X-ray diffraction (XRD) analysis is carried out on the hardfacing surface using X-Ray diffractometer with $\text{Cu K}\alpha$ (1.5405 \AA) radiation and 90° maximum diffraction angle (θ) to identify various phases formed in the hardfacing. Optical microscope (OM) and scanning electron microscope (SEM) are used to analyze the

microstructure of the specimens and Vilella's etchant (5 ml HCL + 1 gm picric acid in 100 ml. ethanol) is used to reveal the microstructure of AISI 4140 and hardfacing materials [24]. Optical microscopy of both the samples is carried out with the magnification of x200. Then the worn surfaces are observed under the SEM to characterize the surface morphology and to establish a possible mechanism for material removal.

3. RESULTS AND DISCUSSIONS

3.1 Analysis of slurry abrasive wear behaviour

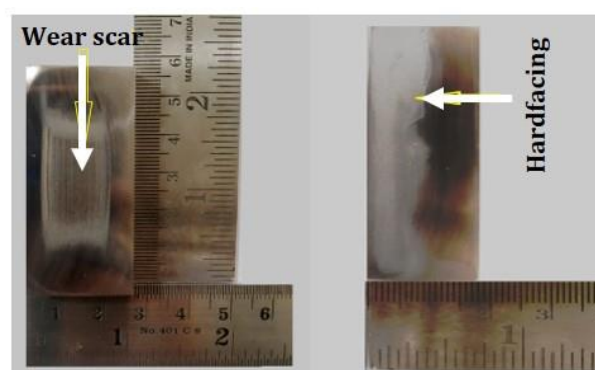


Fig. 7. Worn-out sample after wear test indicating wear scar and hardfacing thickness

Fig. 7. Shows worn-out sample after slurry abrasive wear test. Calculations for mass loss by least-square line for all the seven samples are plotted against different thicknesses of hardfaced materials as presented in Fig. 8. H1-1 and H2-1 samples have wear losses considerably low as compared to the substrate material. Sample H2-1 has shown highest wear resistance whereas H2-3 has shown lowest wear resistance for H2 hardfacing and similar results are obtained for H1 hardfacing. Therefore, it can be seen that the wear loss increases with increase in the thickness of hardfaced surface. When H1 hardfacing compared with H2 hardfacing with reference to each layer, it is observed that H2 hardfacing shows lower mass loss as compared to H1 hardfacing at all the three layers. Hence, it can be concluded that H2 hardfacing provides higher wear resistance as compared to H1 hardfacing which subsequently gives a higher operating time to the roller as compared to H1 hardfacing. As a result of this, the H2 hardfacing significantly reduces the life-cycle cost of hot strip mill rolls by increasing roller life and reducing roll refurbishment costs.

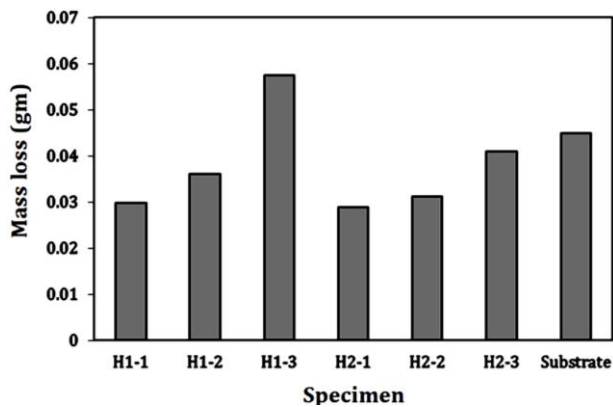


Fig. 8. Slurry abrasive wear loss at different thicknesses

In order to justify the change in wear behaviour of different samples, an in-depth analysis of hardness and microstructural changes are performed as explained in the subsequent sections.

3.2 Analysis of hardness

Fig. 9 shows the schematic diagram of sample for hardness test and Fig. 10 shows hardness profiles of hardfaced samples with different hardfacing materials.

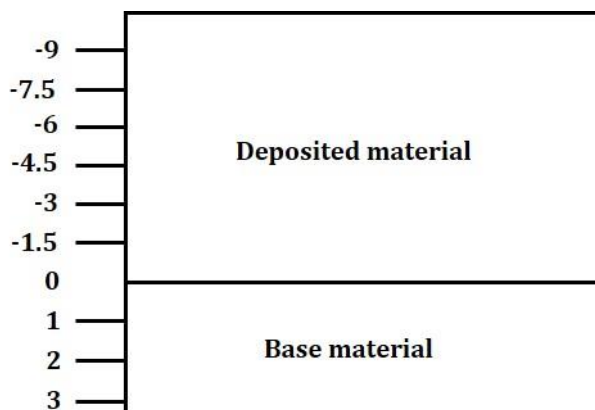


Fig. 9. Schematic diagram of sample for hardness test

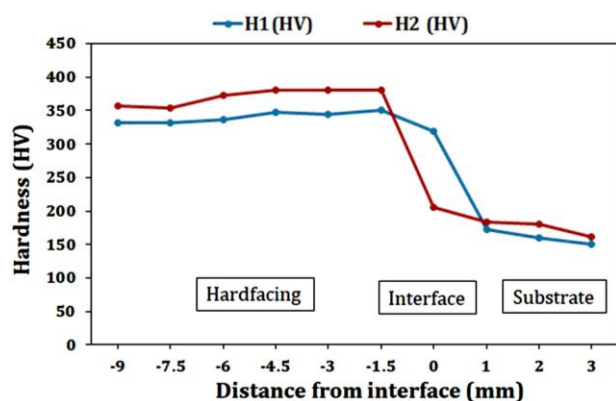


Fig. 10. Hardness profile of both hardfacing materials at different thicknesses

Three distinct zones are appeared in hardness profile viz. substrate zone, interface zone and hardfacing zone. At substrate zone, the hardness of substrate was measured as about 160 HV. The hardness profile for both the materials showed an increasing trend from the top surface to the interface zone which afterward showed decreasing trend from the interface to the substrate material [25]. Peak hardness for H2 is 380 HV and in case of H1 it is 351 HV. Both the hardfacing samples showed the hardness value higher than the substrate material. Hence, during the working of a hardfaced roller, there are less chances of failure of the roller. Therefore, both the hardfaced materials provide a better working applicability as compared to the traditionally manufactured rollers.

3.3 Microstructural analysis

XRD analysis is used to identify the crystalline phases present in both the hardfaced samples. Fig. 11 shows the results of the XRD analysis. XRD peaks of both the hardfaced samples indicate the presence of single martensitic phase. It is noteworthy that the martensite and ferrite peaks are too close to be resolved as separate diffraction lines because of low carbon content of these hardfacing materials. Thus, in hardfaced specimens, the observed peaks may signify a combination of α -Fe and martensite [26]. Other than these phases, no peaks are observed to express the formation of carbide precipitation in hardfacing and heat affected zone. In the fast-cooling process, there is not enough time to form carbide precipitation. But, PWHT process produces tempered martensite which is accepted as an ideal combination of strength and toughness for hot strip mill roller. Also, during PWHT, there is enough time to form carbide precipitation even though their presence is not detected in the results of the XRD analysis, their presence is observed in SEM examinations which indicates that the amount of such precipitation is below 5%. It has been reported that small precipitations that form at amounts below 5% cannot be identified by the XRD pattern [27].

The microstructures of both the hardfaced samples have been examined with OM and SEM. It is observed that the microstructure of hardfacing significantly influences the wear resistance while phases and grain sizes in the microstructure are key factors that considerably affect the mechanical properties.

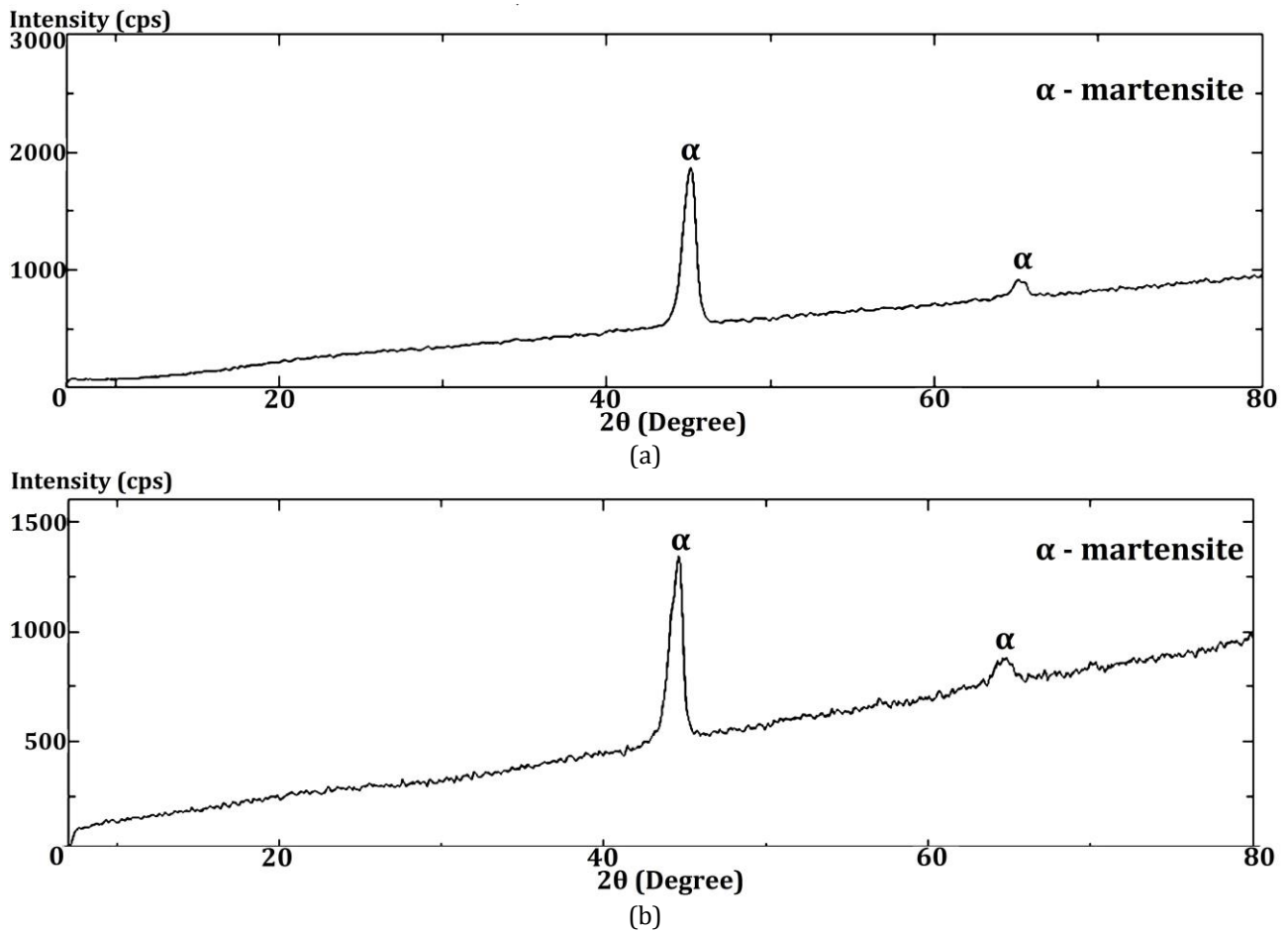
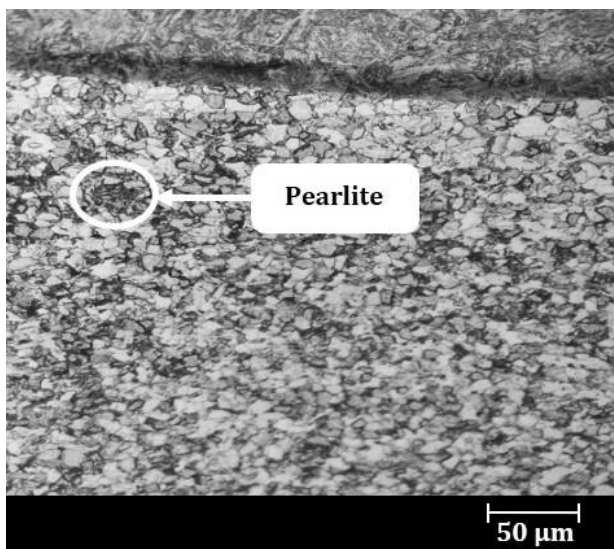


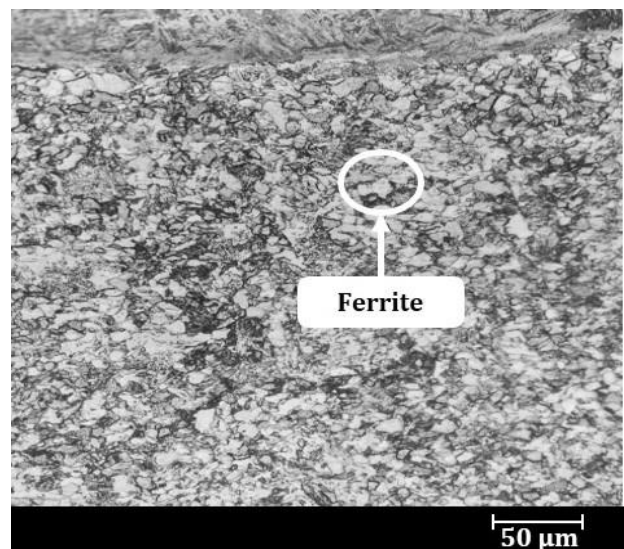
Fig. 11. X-ray patterns for hardfacing of H1 sample (a) and H2 sample (b)

The microstructure of substrate material is shown in Fig. 12 (a) and 12 (b) which consist of polygonal ferrite (white phase) and pearlite (black phase) grains as similarly reported by Deen et al. [28]. It is observed that the grain size of heat affected zone is coarser in comparison to the zone away from the intermediate zone. Fig. 12 (c) and 12 (d) shows the

microstructure of the H1-1 and H2-1 deposited hardfacings respectively. Both the hardfacing materials are low carbon Fe-C alloys. Due to this, it shows two main phases in hardfacing metal, i.e., lath martensite (black portion) and retained austenite (white portion) [29-31].



(a)



(b)

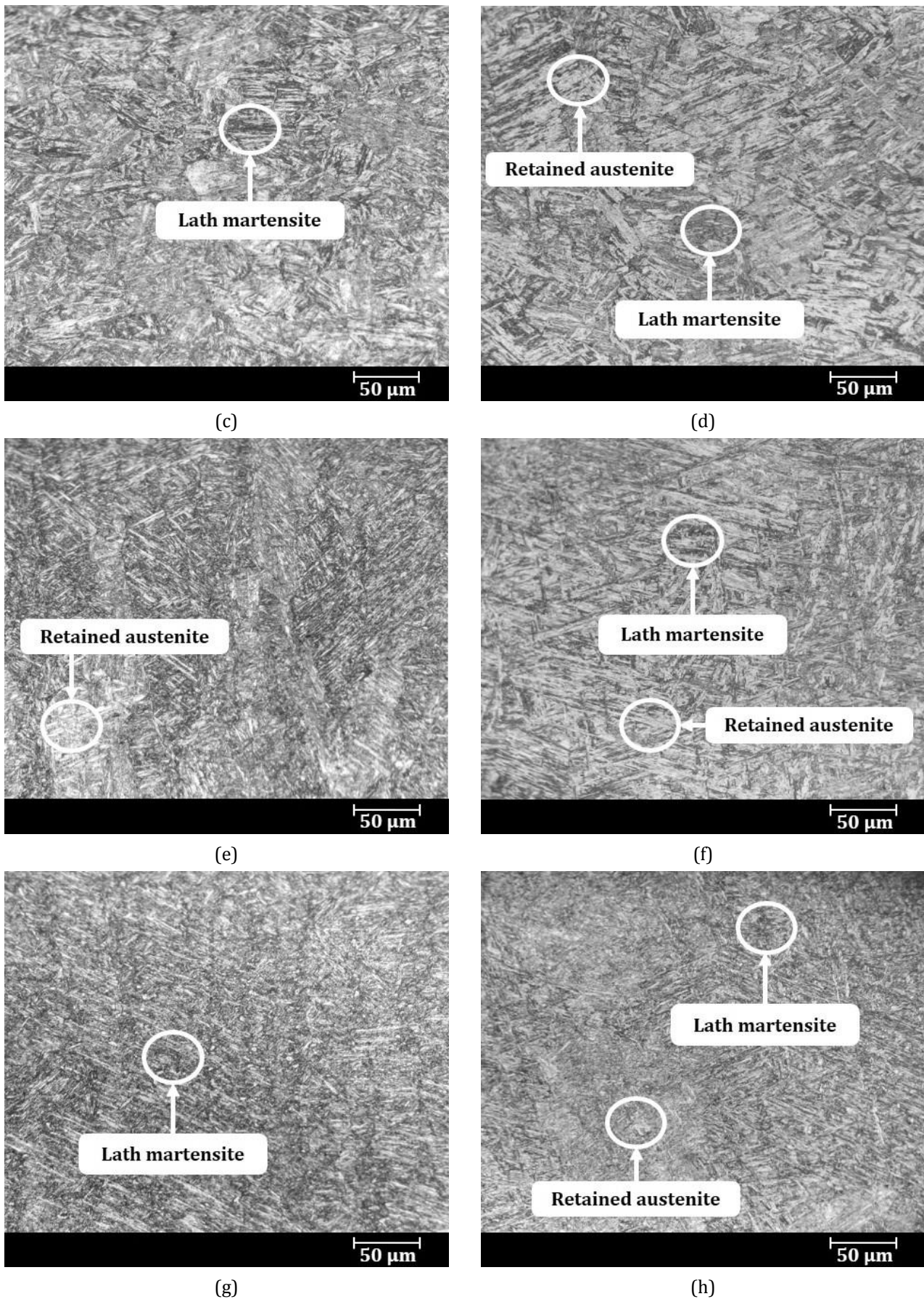


Fig. 12. Optical micrograph of specimens at 200x (a) H1-substrate, (b) H2-substrate, (c) H1-1, (d) H2-1, (e) H1-2, (f) H2-2, (g) H1-3, (h) H2-3

Fig. 12 (e), 12 (f), 12 (g) and 12 (h) also shows two main phases in the hardfacing metal, i.e. lath martensite and retained austenite. Here, from the images of optical microscopy, it is clearly observed that layer 3 has a finer lath martensite phase as compare to layer 1. E. Badisch and C. Mitterer [32] were observe that the coarser phase of lath martensite and retained austenite has a lower wear mass loss as compare to finer phase. Similarly, layer 1 with coarser phase structure shows lower wear mass loss in wear test results as compare to layer 3.

Substrate material has 0.4% C whereas H1 and H2 have 0.08% C and 0.05% C respectively. So, during hardfacing of first layer, because of substrate material dilutes with H1, the proportional amount of carbon in the first layer increases as compare to final layer. As a result of this, H1-1 and H2-1 have a higher hardness and wear resistance property as compare to H1-3 and H2-3 [33]. H1 hardfacing consisted of a higher percentage of Ni in comparison to H2 hardfacing. As Ni forms austenite, it increases the volume of retained austenite in the material. A higher percentage of Ni decreases the hardness of H1 material in comparison to H2 which is similarly reported by Mirzaee et al. [34]. Another alloying element is Mo, which has a major influence on the hardness of a material. Here, the H2 hardfacing is consisted of 150% more Mo in comparison to H1 which provides higher hardness as similarly reported by Ferreira et al. [35]. Both the materials have N and Mo, which form NC and MoC carbides. Vanadium is an extra alloy in H2 hardfacing which forms VC and gives a harder phase to the material.

Fig. 13 shows the results of EDS analysis. Table 2 shows the mass percentage of

elements at specific point. At all specified points in Fig. 13, the percentage of chromium and iron are significantly higher than other elements. Hence, the precipitate form in hardfacing samples might be Fe/Cr carbide [36]. The SEM micrograph of hardfacing materials are shown in Fig. 14. A large volume of fine-sized carbide particles is presented in the hardfacing of H2 wire as shown in Fig. 14 (a). While in the H1 hardfacing, a small volume of carbide phase with coarse size is found on the grain boundaries as shown in Fig. 14 (d). The formation of carbide phase can be found more in H2 hardfacing in comparison to H1. The micrographs of the hardfacing samples revealed lath martensite, retained austenite and carbide precipitates as shown in Fig. 14 (c). As observed from the microstructure, a few portions of the martensitic structures have been transformed to ferrite and other carbides [37]. The size of carbide formed in H1 hardfaced samples can be found larger than H2 samples as shown in Fig. 14 (c) and Fig. 14 (f).

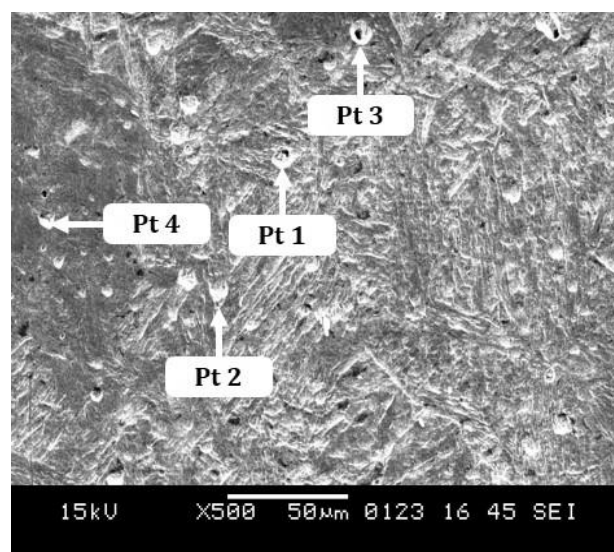


Fig. 13 SEM image of the hardfaced sample

Table 2. Normal mass percentage of elements measured by EDS

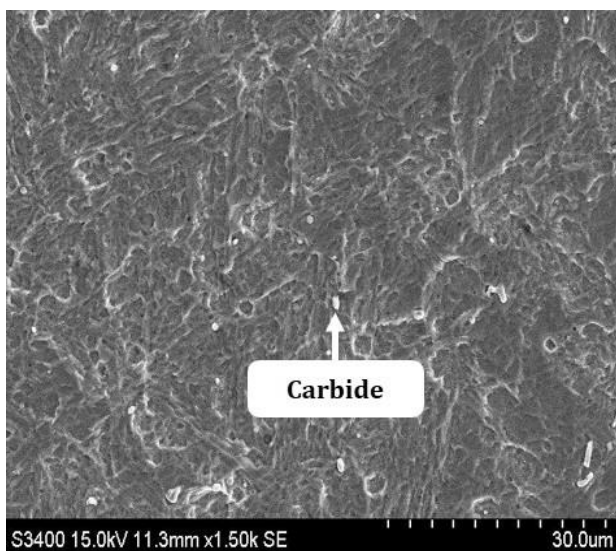
Element	C	N	O	Na	Mg	Al	Si	P	S	Cl	Ca	Cr	Fe	Co	Mo
Pt 1	0.11	-	0.37	-	-	0.83	-	-	-	-	0.20	26.96	66.72	4.80	-
Pt 2	0.81	-	-	-	-	-	0.25	-	0.26	-	-	8.99	89.69	-	-
Pt 3	6.81	-	1.69	0.08	0.13	-	0.21	-	-	-	0.12	33.35	54.88	-	2.79
Pt 4	5.61	-	1.49	-	-	0.23	0.58	-	0.86	-	0.03	15.72	75.48	-	-

From the above discussion, H2 hardfacing showed higher hardness and higher wear resistance in comparison to H1. Hence, H2 hardfaced rollers are more suitable for working conditions of hot strip mill in comparison to H1 hardfaced rollers.

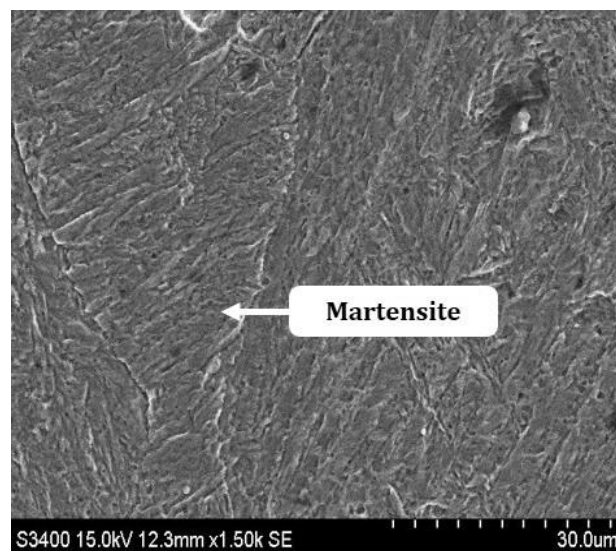
3.4 Analysis of worn-out morphology

In order to correlate the obtained wear characteristics, an in-depth study of a worn-out surface is also attempted with SEM. The specimen which exhibits the lowest wear resistance is selected for this purpose as represented in Fig. 14.

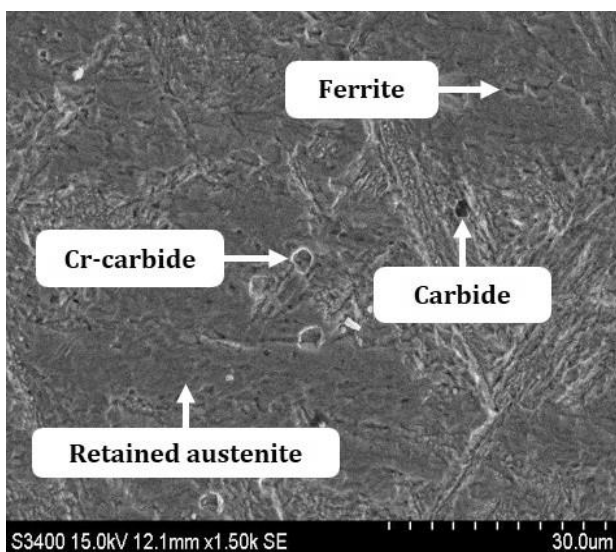
The martensite structure formed in hardfacing material does not indicate that the morphology of samples under the slurry abrasion test give crack or fracture. The microstructure of different layers is shown in Fig. 12 and Fig. 14. It was observed that as thickness of hardfacing increases, the finer size of martensite and carbide are formed. Also, the wear test data indicates that the finer phases of martensite and carbides are resulted into relatively higher abrasion wear mass loss as compared to coarser martensite and carbides as similarly reported by E. Badisch and C. Mitterer [32].



(a)



(b)



(c)



(d)

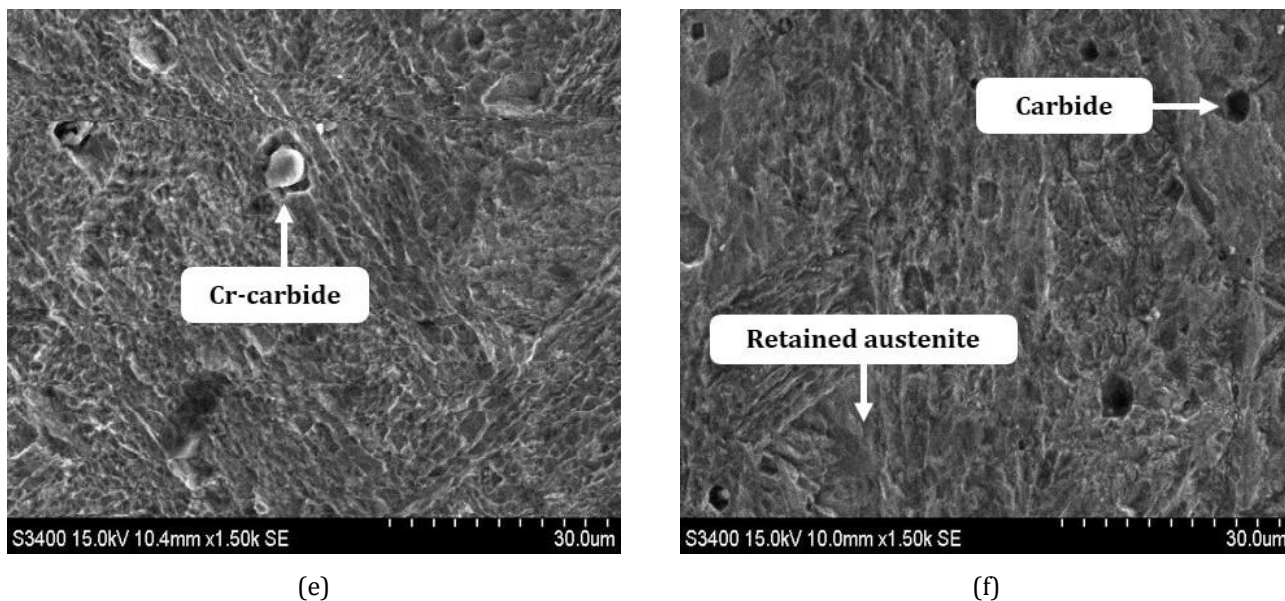


Fig. 14. SEM micrograph of specimens (a) H2-3, (b) H2-2, (c) H2-1, (d) H1-3, (e) H1-2, (f) H1-1

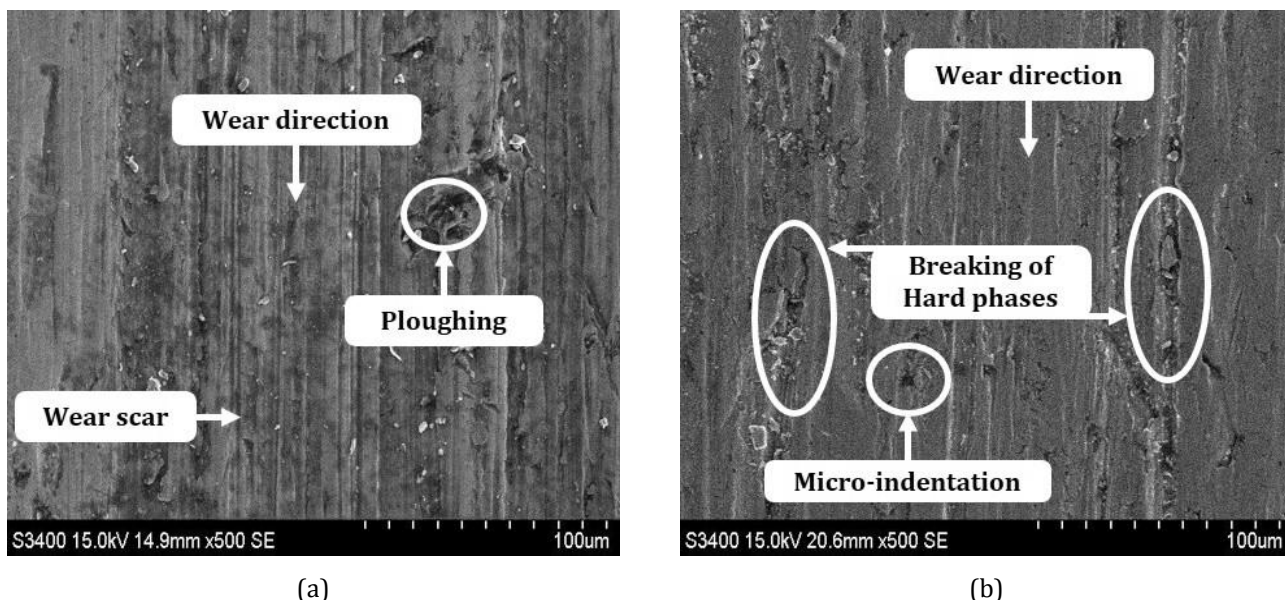


Fig. 15. SEM images of worn-out surface of (a) H2 hardfacing (b) H1 hardfacing

Fig. 15 shows severe grooving of the surface with scratches lying parallel to each other and in the direction of slurry flow can be observed. Also, because of detached asperities from the hardfacing surface, pits are formed on the worn surface. The principal material removal mechanism is observed as abrasive wear and plastic flow. Fig. 15 (a) shows a uniform abrasive wear across the surface along with some ploughing due to the detached metal participation in the subsequent wear. The materials, removed by microploughing, show that specimen (a) has higher hardness and lower wear loss in comparison to specimen (b) [38]. Fig. 15 (b) shows the morphology of worn-out

surface which indicates the susceptibility of martensitic microstructure either to crack or to fracture under given slurry abrasion conditions. Breaking of hard particles such as carbides and nitride at some places leave behind micro-cracks and fractures at severe points. Hence, the main wear mechanism is abrasive wear with little plastic flow due to detached metal particles. These wear mechanisms on the macro-scale show little roughness to touch on the roller surface. As a result of this, it deteriorates the quality of hot-rolled products during the rolling process. Therefore, periodical dressing of hardfaced surface is carried out to maintain the quality of mill products.

4. CONCLUSIONS

The martensitic stainless-steel hardfacing alloys are deposited on AISI 4140 using SAW process. Good bonding between substrate material and hardfacing material is obtained without any surface cracks or lack of adhesion. Deposition characteristics such as an average hardfacing thickness, the microstructure of hardfaced sample with a SEM, hardness profile, slurry abrasive wear test and worn-out morphology are analyzed. Following observations are laid down:

- Slurry abrasive wear test results shows that H2 hardfacing provides better wear resistance compared to H1 hardfacing.
- Metallographic investigations showed that with the increasing number of hardfacing layers, the volume of retained austenite also increases which leads to lower down the hardness of subsequent hardfacing layers.
- It is observed that the third layer of H1 hardfacing shows higher wear mass loss as compared to the substrate and the third layer in case of H2 hardfacing shows lesser wear mass loss as compared to the substrate. Hence, it is suggested that two layers are beneficial for H1 hardfacing whereas three layers are for H2 hardfacing to obtain better characteristics of the hardfacing layer as compared to the substrate.
- The value of hardness is highest at the first layer and it decreases as the number of hardfacing layers increases.
- With the increase of molybdenum, nickel, and vanadium in the hardfacing, wear resistance also increases.

Overall observations from the present work show that the hardfacing of H2 welding wire gives a better wear resistance property in comparison to H1 welding wire for the same number of hardfacing layers. The H2 wire significantly reduces the life-cycle cost of hot strip mill roller by increasing roller life and reducing roller refurbishment costs. Therefore, H2 hardfacing is suggested for reconditioning of worn-out hot strip mill roller made up of AISI 4140 substrate material.

Acknowledgement

The authors would like to acknowledge Arcelormittal Nippon Steel, Hazira, India for providing all the facilities for carrying out the experiments and testing at their work site.

REFERENCES

- [1] S. Matthews, B. James, *Review of Thermal Spray Coating Applications in the Steel Industry: Part 1—Hardware in Steel Making to the Continuous Annealing Process*, Journal of Thermal Spray Technology, vol. 19, no. 6, pp. 1267-1276, 2010, doi: [10.1007/s11666-010-9518-8](https://doi.org/10.1007/s11666-010-9518-8)
- [2] A. Sanz, *New coatings for continuous casting rolls*, Surface and Coatings Technology, vol. 177-178, pp. 1-11, 2004, doi: [10.1016/j.surfcoat.2003.06.024](https://doi.org/10.1016/j.surfcoat.2003.06.024)
- [3] E.N. Shebanits, N.I. Omelyanenko, Y.N. Kurakin, V.N. Matvienko, L.K. Leshchinskii, B.E. Dubinskii, K.K. Stepnov, *Improving the fracture toughness and wear resistance of hard-faced hot-rolling-mill rolls*, Metallurgist, vol. 56, no. 7-8, pp. 613-617, 2012, doi: [10.1007/s11015-012-9623-7](https://doi.org/10.1007/s11015-012-9623-7)
- [4] Y.T. Qi, Z.D. Zou, *Microstructure and wear properties of laser coating reinforced by Ti (CxN1-x) on adamite roller*, Journal of Iron and Steel Research, International, vol. 16, no. 3, pp. 78-82, 2009, doi: [10.1016/S1006-706X\(09\)60048-0](https://doi.org/10.1016/S1006-706X(09)60048-0)
- [5] K. Yang, Z.X. Zhang, W.Q. Hu, Y.F. Bao, Y.F. Jiang, *A new type of submerged-arc flux-cored wire used for hardfacing continuous casting rolls*, Journal of Iron and Steel Research, International, vol. 18, no. 11, pp. 74-79, 2011, doi: [10.1016/S1006-706X\(11\)60120-9](https://doi.org/10.1016/S1006-706X(11)60120-9)
- [6] A. Ray, K.S. Arora, S. Lester, M. Shome, *Laser cladding of continuous caster lateral rolls: Microstructure, wear and corrosion characterisation and on-field performance evaluation*, Journal of Materials Processing Technology, vol. 214, iss. 8, pp. 1566-1575, 2014, doi: [10.1016/j.jmatprotec.2014.02.027](https://doi.org/10.1016/j.jmatprotec.2014.02.027)
- [7] V.E. Buchanan, P.H. Shipway, D.G. McCartney, *Microstructure and abrasive wear behaviour of shielded metal arc welding hardfacings used in the sugarcane industry*, Wear, vol. 263, iss. 1-6, pp. 99-110, 2007, doi: [10.1016/j.wear.2006.12.053](https://doi.org/10.1016/j.wear.2006.12.053)
- [8] A.K. Gur, C. Ozay, B. Icen, *Evaluation of b4c/ti coating layer, investigation of abrasive wear behaviors using taguchi technique and response surface methodology*, Surface Review and Letters, vol. 27, no. 10, pp. 1950225-1-1950225-17, 2020, doi: [10.1142/S0218625X19502251](https://doi.org/10.1142/S0218625X19502251)
- [9] S. Taskaya, A.K. Gur, C. Ozay, *Joining of Ramor 500 Steel with SAW (Submerged Arc Welding)*

- and its Evaluation of Thermomechanical Analysis in ANSYS Package Software, Thermal Science and Engineering Progress, vol. 13, pp. 100396-1-100396-16, 2019, doi: [10.1016/j.tsep.2019.100396](https://doi.org/10.1016/j.tsep.2019.100396)
- [10] S. Taskaya, A.K. Gur, A. Orhan, *Joining of Ramor 500 Steel by Submerged Welding and its Examination of Thermal Analysis in ANSYS Package Program*, Thermal Science and Engineering Progress, vol. 11, pp. 84-110, 2019, doi: [10.1016/j.tsep.2019.02.002](https://doi.org/10.1016/j.tsep.2019.02.002)
- [11] J. Vinas, J. Brezinova, A. Guzanova, J. Svetlik, *Degradation of renovation layers deposited on continuous steel casting rollers by submerged arc welding*, Proceedings of the Institution of Mechanical Engineers, Part B: Journal of Engineering Manufacture, vol. 227, iss. 12, pp. 1841-1848, 2013, doi: [10.1177/0954405413493405](https://doi.org/10.1177/0954405413493405)
- [12] M. Du Toit, J. Van Niekerk, *Improving the life of continuous casting rolls through submerged arc cladding with nitrogen-alloyed martensitic stainless steel*, Welding in the World, vol. 54, no. 11-12, pp. R342-R349, 2010, doi: [10.1007/BF03266748](https://doi.org/10.1007/BF03266748)
- [13] A. Farzadi, R. Kalantarian, *Microstructural development and corrosion behavior of 13Cr-4Ni-1Mo martensitic stainless steel clad*, Welding in the World, vol. 64, no. 11, pp. 1811-1823, 2020, doi: [10.1007/s40194-020-00961-9](https://doi.org/10.1007/s40194-020-00961-9)
- [14] S. Zhang, P. Wang, D. Li, Y. Li, *Investigation of the evolution of retained austenite in Fe-13% Cr-4% Ni martensitic stainless steel during intercritical tempering*, Materials and Design, vol. 84, pp. 385-394, 2015, doi: [10.1016/j.matdes.2015.06.143](https://doi.org/10.1016/j.matdes.2015.06.143)
- [15] M. Ulutan, M.M. Yildirim, S. Buytoz, O.N. Celik, *Microstructure and wear behavior of tig surface-alloyed AISI 4140 steel*, Tribology Transactions, vol. 54, iss. 1, pp. 67-79, 2010, doi: [10.1080/10402004.2010.519859](https://doi.org/10.1080/10402004.2010.519859)
- [16] S.H. Choo, S. Lee, M.G. Golkovski, *Effects of accelerated electron beam irradiation on surface hardening and fatigue properties in an AISI 4140 steel used for automotive crankshaft*, Materials Science and Engineering: A, vol. 293, iss. 1-2, pp. 56-70, 2000, doi: [10.1016/S0921-5093\(00\)01207-7](https://doi.org/10.1016/S0921-5093(00)01207-7)
- [17] A. Medina-Flores, J. Oseguera, P. Santiago, J.A. Ascencio, *Structural analysis of AISI-SAE 4140 steel nitrated by post-discharge microwave*, Surface and Coatings Technology, vol. 188-189, pp. 7-12, 2004, doi: [10.1016/j.surfcoat.2004.07.092](https://doi.org/10.1016/j.surfcoat.2004.07.092)
- [18] A.H. Meysami, R. Ghasemzadeh, S.H. Seyedein, M.R. Aboutalebi, *An investigation on the microstructure and mechanical properties of direct-quenched and tempered AISI 4140 steel*, Materials and Design, vol. 31, iss. 3, pp. 1570-1575, 2010, doi: [10.1016/j.matdes.2009.09.040](https://doi.org/10.1016/j.matdes.2009.09.040)
- [19] M.A. Hafeez, A. Farooq, *Effect of heat treatments on the mechanical and electrochemical corrosion behavior of 38CrSi and AISI 4140 steels*, Metallography, Microstructure, and Analysis, vol. 8, no. 4, pp. 479-487, 2019, doi: [10.1007/s13632-019-00556-x](https://doi.org/10.1007/s13632-019-00556-x)
- [20] K. Yang, S. Yu, Y. Li, C. Li, *Effect of carbonitride precipitates on the abrasive wear behaviour of hardfacing alloy*, Applied Surface Science, vol. 254, iss. 16, pp. 5023-5027, 2008, doi: [10.1016/j.apsusc.2008.01.154](https://doi.org/10.1016/j.apsusc.2008.01.154)
- [21] R. Puli, G.D.J. Ram, *Wear and corrosion performance of AISI 410 martensitic stainless steel coatings produced using friction surfacing and manual metal arc welding*, Surface and Coatings Technology, vol. 209, pp. 1-7, 2012, doi: [10.1016/j.surfcoat.2012.06.075](https://doi.org/10.1016/j.surfcoat.2012.06.075)
- [22] O. Maranhao, D. Rodrigues, M. Boccalini Jr., A. Sinatora, *Mass loss and wear mechanisms of HVOF-sprayed multi-component white cast iron coatings*, Wear, vol. 274-275, pp. 162-167, 2012, doi: [10.1016/j.wear.2011.08.024](https://doi.org/10.1016/j.wear.2011.08.024)
- [23] J.D.B. De Mello, A.A. Polycarpou, *Abrasive wear mechanisms of multi-components ferrous alloys abraded by soft, fine abrasive particles*, Wear, vol. 269, iss. 11-12, pp. 911-920, 2010, doi: [10.1016/j.wear.2010.08.025](https://doi.org/10.1016/j.wear.2010.08.025)
- [24] A.D. Anjos, C.J. Scheuer, S.F. Brunatto, R.P. Cardoso, *Low-temperature plasma nitrocarburizing of the AISI 420 martensitic stainless steel: microstructure and process kinetics*, Surface and Coatings Technology, vol. 275, pp. 51-57, 2015, doi: [10.1016/j.surfcoat.2015.03.039](https://doi.org/10.1016/j.surfcoat.2015.03.039)
- [25] N.V. Rao, G.M. Reddy, S. Nagarjuna, *Weld overlay cladding of high strength low alloy steel with austenitic stainless steel-structure and properties*, Materials and Design, vol. 32, iss. 4, pp. 2496-2506, 2011, doi: [10.1016/j.matdes.2010.10.026](https://doi.org/10.1016/j.matdes.2010.10.026)
- [26] B.A. Tabatabae, F. Ashrafizadeh, A.M. Hassanli, *Influence of retained austenite on the mechanical properties of low carbon martensitic stainless steel castings*, ISIJ International, vol. 51, iss. 3, pp. 471-475, 2011, doi: [10.2355/isijinternational.51.471](https://doi.org/10.2355/isijinternational.51.471)
- [27] C. Kose, R. Kacar, *The Effect of Preheat & Post Weld Heat Treatment on the Laser Weldability of AISI 420 Martensitic Stainless Steel*, Materials and Design, vol. 64, pp. 221-226, 2014, doi: [10.1016/j.matdes.2014.07.044](https://doi.org/10.1016/j.matdes.2014.07.044)
- [28] K.M. Deen, R. Ahmad, I.H. Khan, Z. Farahat, *Microstructural study and electrochemical behavior of low alloy steel weldment*, Materials and Design, vol. 31, iss. 6, pp. 3051-3055, 2010, doi: [10.1016/j.matdes.2010.01.025](https://doi.org/10.1016/j.matdes.2010.01.025)
- [29] B. Abbasi-Khazaei, A. Mollaahmadi, *Rapid Tempering of Martensitic Stainless Steel AISI420: Microstructure, Mechanical and Corrosion*

- Properties*, Journal of Materials Engineering and Performance, vol. 26, no. 4, pp. 1626-1633, 2017, doi: [10.1007/s11665-017-2605-y](https://doi.org/10.1007/s11665-017-2605-y)
- [30] K.H. Anantha, C. Ornek, S. Ejnermark, A. Medvedeva, J. Sjostrom, J. Pan, *Correlative Microstructure Analysis and In Situ Corrosion Study of AISI 420 Martensitic Stainless Steel for Plastic Molding Applications*, Journal of The Electrochemical Society, vol. 164, no. 4, pp. C85-C93, 2017, doi: [10.1149/2.0531704jes](https://doi.org/10.1149/2.0531704jes)
- [31] L.A. Norstrom, *The relation between microstructure and yield strength in tempered low-carbon lath martensite with 5% nickel*, Metal Science, vol. 10, iss. 12, pp. 429-436, 1976, doi: [10.1179/030634576790431868](https://doi.org/10.1179/030634576790431868)
- [32] E. Badisch, C. Mitterer, *Abrasive wear of high speed steels: influence of abrasive particles and primary carbides on wear resistance*, Tribology International, vol. 36, iss. 10, pp. 765-770, 2003, doi: [10.1016/S0301-679X\(03\)00058-6](https://doi.org/10.1016/S0301-679X(03)00058-6)
- [33] L.E.H.S. Rivero, A. Pizzatto, M.F. Teixeira, A. Rabelo, T. Falcade, A. Scheid, *Effect of laser power and substrate on the Hastelloy C276™ coatings features deposited by laser cladding*. Material Research, vol. 23, no. 2, pp. 1-11, 2020, doi: [10.1590/1980-5373-mr-2020-0067](https://doi.org/10.1590/1980-5373-mr-2020-0067)
- [34] M. Mirzaee, A. Momeni, N. Aieni, H. Keshmiri, *Effect of quenching and tempering on microstructure and mechanical properties of 410 and 410 Ni martensitic stainless steels*, Journal of Materials Research, vol. 32, iss. 3, pp. 687-696, 2017, doi: [10.1557/jmr.2016.485](https://doi.org/10.1557/jmr.2016.485)
- [35] L.M. Ferreira, S.F. Brunatto, R.P. Cardoso, *Martensitic stainless steels low-temperature nitriding: dependence of substrate composition*. Materials Research, vol. 18, no. 3, pp. 622-627, 2015, doi: [10.1590/1516-1439.015215](https://doi.org/10.1590/1516-1439.015215)
- [36] M. Kirchgaßner, E. Badisch, F. Franek, *Behaviour of iron-based hardfacing alloys under abrasion and impact*, Wear, vol. 265, iss. 5-6, pp. 772-779, 2008. doi:[10.1016/j.wear.2008.01.004](https://doi.org/10.1016/j.wear.2008.01.004)
- [37] J.C. Ezechidelu, S.O. Enibe, D.O. Obikwelu, P.S. Nnamchi, C.S. Obayi, *Effect of heat treatment on the microstructure and mechanical properties of a welded AISI 410 martensitic stainless steel*, International Advanced Research Journal in Science, Engineering and Technology, vol. 3, iss. 4, pp. 6-12, 2016, doi: [10.17148/IARJSET.2016.3402](https://doi.org/10.17148/IARJSET.2016.3402)
- [38] S.G. Sapate, A.D. Chopde, P.M. Nimbalkar, D.K. Chandrakar, *Effect of microstructure on slurry abrasion response of En-31 steel*, Materials and Design, vol. 29, iss. 3, pp. 613-621, 2008, doi: [10.1016/j.matdes.2007.02.014](https://doi.org/10.1016/j.matdes.2007.02.014)